My Research Interests related to Planetary Physics

Keke ZHANG

Department of Mathematical Sciences

Center for Geophysical and Astrophysical Fluid Dynamics

University of Exeter

5 December, Exeter

UNIVERSITY OF EXETER

School of Engineering, Computer Science and Mathematics

Research Interests

(1) Theoretical problems in rotating fluids

(2) Atmospheric dynamics of planets

(3) Planetary dynamo problems

Outline: Three examples

(1) Convective instabilities in rotating spherical systems:
asymptotic solutions (JFM, 2007)

(2) Mean flow in Jupiter:
saturation of the inverse cascade process (ApJ, 2007)

(3) Planetary dynamos: a new generation model (PEPI 2007)

Asymptotic solutions of thermal convection

The problem of convective instabilities/flows, which generate small-scale vortices in rotating spherical systems, is a classical problem

Chandrasekhar, (1961, monograph);
Roberts, (1968, Proc. Roy. Soc.);
Busse, (1970 J. Fluid Mech.);
Soward, (1977, GAFD)
Zhang (1992, J. Fluid Mech.);
Jones et al. (2000, J. Fluid Mech.)...

We report asymptotic solutions of convection with the no-slip boundary condition in rapidly rotating spherical systems, valid for $0 \leq P_r/E < \infty$ at an arbitrarily small but fixed $E \ll 1$ (Zhang et al., 2007, JFM).

Asymptotic solutions

Convective instabilities/flows in rapidly rotating spherical systems.

Sketch of geometry (Chandrasekhar, 1961):

- Radial Gravity: $\mathbf{g} = -\gamma\mathbf{r}$.
- Unstable Temp. Gradient: $\nabla T_0(r) = -\beta\mathbf{r}$.

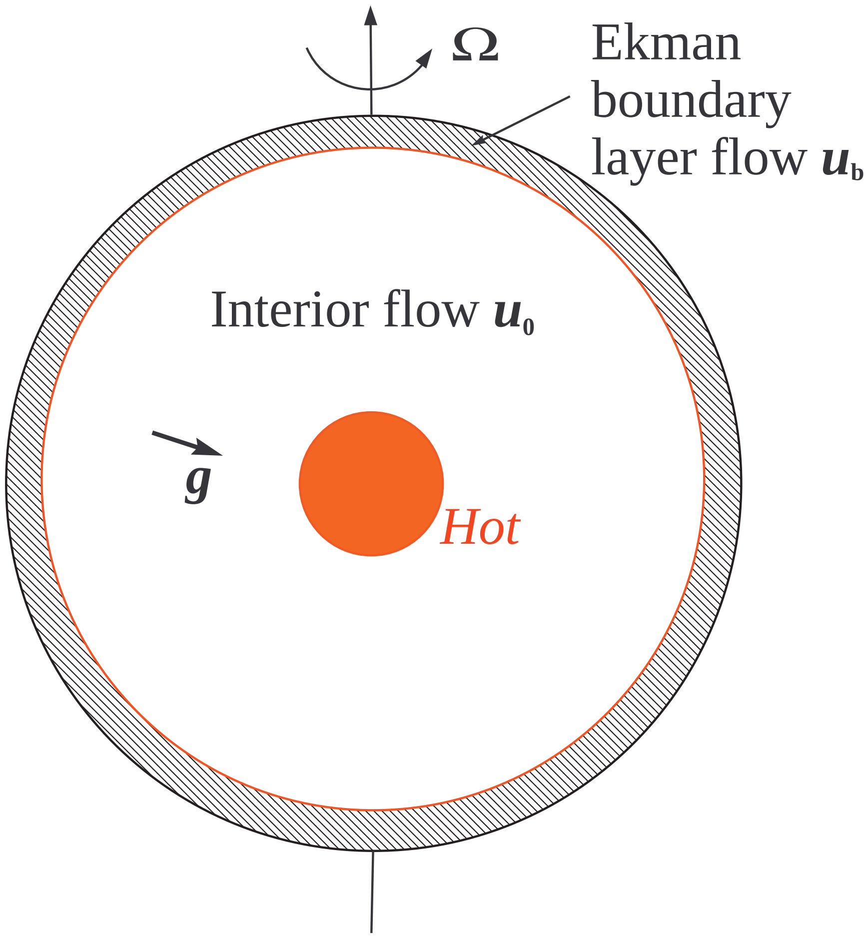

Governing equations

The problem of convective instabilities is governed by the three dimensionless equations

$$\frac{\partial \mathbf{u}}{\partial t} + \mathbf{u} \cdot \nabla \mathbf{u} + 2\mathbf{k} \times \mathbf{u} = -\nabla p + R\Theta\mathbf{r} + E\nabla^2\mathbf{u}, \tag{1}$$

$$(P_r/E)\left(\frac{\partial \Theta}{\partial t} + \mathbf{u} \cdot \nabla\Theta\right) = \mathbf{u} \cdot \mathbf{r} + \nabla^2\Theta, \tag{2}$$

$$\nabla \cdot \mathbf{u} = 0, \tag{3}$$

where $\mathbf{k}$ is a unit vector parallel to the axis of rotation and

$$R = \frac{\alpha\beta\gamma r_o^4}{\Omega\kappa},\ P_r = \frac{\nu}{\kappa},\ E = \frac{\nu}{\Omega r_o^2}.$$

The rigid, no-slip boundary with fixed temperature gives

$$u_r = u_\theta = u_\phi = \Theta = 0 \ \text{ at } \ r = r_0. \tag{4}$$

Interior Solutions

The asymptotic solution of the interior flow $\mathbf{u}_0$ at $E \to 0$ is expressed as

$$\mathbf{u}_0 = \sum_N C_N \left(\mathbf{U}_N + \tilde{\mathbf{u}}_N\right)\ e^{2\mathrm{i}\sigma t}, \quad \mathbf{p}_0 = \sum_N C_N \left(P_N + \tilde{p}_N\right)\ e^{2\mathrm{i}\sigma t}, \tag{5}$$

where $\tilde{\mathbf{u}}_N$ denotes perturbations induced by the flux from the Ekman layer and $\mathbf{U}_N$ is solutions of

$$2\left(\mathbf{i}\sigma_N \mathbf{U}_N + \mathbf{k} \times \mathbf{U}_N\right) + \nabla P_N = 0, \quad \nabla \cdot \mathbf{U}_N = 0, \tag{6}$$

subject to $\hat{\mathbf{r}} \cdot \mathbf{U}_N = 0$ at $r = r_0$. Explicit expressions for all $\mathbf{U}_N$ was found by Zhang et al (JFM, 2004). The interior flow $\mathbf{u}_0$ is characterized by

$$\hat{\mathbf{r}} \cdot \mathbf{u}_0 = O(E^{1/2}), \tag{7}$$

which is required in the process of asymptotic matchings for the higher-order problem.

An important property of the interior solution

The interior flow u_0 is represented by a new Poincaré polynomial associated with the Poincaré equation found by Zhang and Liao (2005). The asymptotic matching requires to evaluate the three-dimensional viscous dissipation integral

$$\int\int\int_V \mathbf{u}_0 \cdot \nabla^2 \mathbf{u}_0 \, dV = S_{1N} + S_{2N} + S_{3N}$$

where

$$S_{1N} \sim \sum_{i=0}^{N} \sum_{k=1}^{N} \sum_{j=0}^{N-i} \sum_{l=0}^{N-k} (-1)^{i+j+k+l} \sigma_{Nmn}^{2(i+k)} (1 - \sigma_{Nmn}^2)^{j+l}$$

$$\frac{[m^2 + (m+2j)(m+2l)][2(m+N+i+j)-1]!!}{[2(l+k+i+j+m)-1]!!}$$

$$\frac{[2(m+N+k+l)-1]!!}{(2i-1)!!(N-i-j)!i!j!(m+j)!(k-1)!l!} \frac{(2i+2k-3)!!(l+j+m-1)!}{(2k-3)!!(l+m)!(N-k-l)!};$$

An important property of the interior solution

$$S_{2N} \sim \sum_{i=0}^{N}\sum_{k=1}^{N}\sum_{j=0}^{N-i}\sum_{l=0}^{N-k}(-1)^{i+j+k+l}\sigma_{Nmn}^{2(i+k)}(1-\sigma_{Nmn}^2)^{j+l}$$

$$\frac{[2(m+N+i+j)-1]!!}{[2(l+k+i+j+m)-1]!!}$$

$$\frac{[2(m+N+k+l)-1]!!}{(2i-1)!!(N-i-j)!i!j!(m+j)!(k-1)!l!}\,\frac{(2i+2k-3)!!(l+j+m)!}{(2k-3)!!(l+m)!(N-k-l)!},$$

$$S_{3N} \sim \sum_{i=1}^{N}\sum_{k=2}^{N}\sum_{j=0}^{N-i}\sum_{l=0}^{N-k}(-1)^{i+j+k+l}\sigma_{Nmn}^{2(i+k)}(1-\sigma_{Nmn}^2)^{j+l}$$

$$\frac{[2(m+N+i+j)-1]!!}{[2(l+k+i+j+m)-1]!!}$$

$$\frac{[2(m+N+k+l)-1]!!}{(2i-1)!!(N-i-j)!(i-1)!j!(m+j)!(k-2)!l!}\,\frac{(2i+2k-5)!!(l+j+m)!}{(2k-3)!!(l+m)!(N-k-l)!}.$$

We have provided the mathematical proof showing that

$$S_{1N} = S_{2N} = S_{3N} \equiv 0 \quad \rightarrow \quad \int\!\!\int\!\!\int_V \mathbf{u}_0 \cdot \nabla^2 \mathbf{u}_0 \, dV \equiv 0.$$

Boundary solutions

For a sufficiently small E, the Ekman boundary flow $\mathbf{u}_b$ is governed by

$$2\mathrm{i}\sigma\mathbf{u}_b + 2\mathbf{k}\times\mathbf{u}_b - \hat{\mathbf{r}}\frac{\partial p_b}{\partial\xi} = \frac{\partial^2\mathbf{u}_b}{\partial\xi^2}, \tag{8}$$

where $\xi = E^{-1/2}(1-r)$, for $E \ll 1$. **It can be reduced to**

$$\left(\frac{\partial^2}{\partial\xi^2} - 2\mathbf{i}\sigma\right)^2\mathbf{u}_b + 4\left(\mathbf{k}\cdot\hat{\mathbf{r}}\right)^2\mathbf{u}_b = 0, \tag{9}$$

subject to four boundary conditions,

$$\left[\mathbf{r}\times\mathbf{u}_b\right]_{\xi=0} + \sum_N C_N\left[\mathbf{r}\times\mathbf{U}_N\right]_{r=1} = 0, \tag{10}$$

$$\left[\frac{\partial^2\mathbf{u}_b}{\partial\xi^2}\right]_{\xi=0} + \sum_N 2C_N\left[\mathbf{i}\sigma\mathbf{U}_N + (\mathbf{k}\cdot\hat{\mathbf{r}})\hat{\mathbf{r}}\times\mathbf{U}_N\right]_{r=1} = 0. \tag{11}$$

$$\left[\hat{\mathbf{r}}\times\hat{\mathbf{u}}_b\right]_{\xi=\infty} = 0, \quad \left[\frac{\partial^2\mathbf{u}_b}{\partial\xi^2}\right]_{\xi=\infty} = 0. \tag{12}$$

Boundary solutions

A cumbersome analysis shows that $\mathbf{u}_b$ at the Ekman boundary layer is

$$\mathbf{u}_b = -\sum_N C_N \left[\frac{B_N^+}{2} \left(\mathbf{i}\hat{\boldsymbol{\theta}} + \hat{\boldsymbol{\phi}} \right) \mathbf{exp} \left(Z_N^+ \xi \right) + \frac{B_N^-}{2} \left(\mathbf{i}\hat{\boldsymbol{\theta}} - \hat{\boldsymbol{\phi}} \right) \mathbf{exp} \left(Z_N^- \xi \right) \right]$$

where

$$\begin{aligned} Z_N^{\pm} &= -\left[1 + \frac{(\sigma_N \pm \cos\theta)}{|\sigma_N \pm \cos\theta|} \mathrm{i} \right] \sqrt{|\sigma_N \pm \cos\theta|}, \\ B_N^{\pm} &= \sum_{i=0}^{N} \sum_{j=0}^{N-i} \frac{C_{ijmN}}{Q_N} \left[\sigma_N^{2i-1} (1-\sigma_N^2)^{j-1} \sin^{m+2j-1}\theta \cos^{2i-1}\theta \right] \\ \times & \left[-\sigma_N (m + m\sigma_N + 2j\sigma_N) \cos^2\theta - 2i(1-\sigma_N^2)\sin^2\theta \right. \\ \pm & \left. \sigma_N (m + m\sigma_N + 2j) \cos\theta \right], \end{aligned}$$

with C_{ijmN} being defined as

$$C_{ijmN} = \frac{(-1)^{i+j}[2(N+i+j+m)-1]!!}{2^{j+1}(2i-1)!!(N-i-j)!i!j!(m+j)!}.$$

The limit $P_r/E \ll 1$

When $P_r/E \ll 1$, we obtain

$$
\begin{aligned}
R &= \frac{E^{1/2}}{\mathcal{G}_{KK}}[\pi \int_0^{\pi} B_K^{+} \frac{(\sigma_K + \cos\theta)}{|\sigma_K + \cos\theta|^{3/2}} (\sin\theta \frac{\partial P_K}{\partial \theta} - m P_K) d\theta + E^{1/2} \mathcal{F}_{KK}], \\
\sigma &= \sigma_K - E^{1/2} \pi \left[\int_0^{\pi} \frac{B_K^{+}}{\sqrt{|\sigma_K + \cos\theta|}} \left(\sin\theta \frac{\partial P_K}{\partial \theta} - m P_K \right) d\theta \right].
\end{aligned}
$$

Minimization of R over different modes, we found the simple asymptotic relation at the convective instabilities,

$$m_c = 1,\ R_c = E^{1/2} \left(8.868 \times 10^2 + 1.033 \times 10^4 E^{1/2} \right),$$

$$\sigma_c = 0.7550 + 0.2177 E^{1/2}.$$

The limit $P_r/E \ll 1$

The explicit asymptotic solution for convection is

$$
\begin{aligned}
u_r &= \mathrm{i}\sin\theta\left[r^2-1\right], \\
u_\phi &= \left[1-2r^2-gr^2(\cos^2\theta-\sin^2\theta)\right]-[(1-\cos\theta)\left(-1-g(\cos^2\theta-\sin^2\theta)/2\right) \\
&\quad +2g\sin^2\theta\cos\theta]e^{(1-r)Z_1^+E^{-1/2}} \\
&\quad -[(1+\cos\theta)\left(-1-g(\cos^2\theta-\sin^2\theta)\right)/2-2g\sin^2\theta\cos\theta]e^{(1-r)Z_1^-E^{-1/2}} \\
u_\theta &= \left[(2-g)\,r^2-1\right]\cos\theta-[(1-\cos\theta)\left(-1-g(\cos^2\theta-\sin^2\theta)\right)/2+ \\
&\quad 2g\sin^2\theta\cos\theta]e^{(1-r)Z_1^+E^{-1/2}}+[(1+\cos\theta)\left(-1-g(\cos^2\theta-\sin^2\theta)\right)/2 \\
&\quad -g\sin^2\theta\cos\theta]e^{(1-r)Z_1^-E^{-1/2}}
\end{aligned}
$$

$$
g\equiv\frac{4\sqrt{10}}{9}-\frac{5}{9},\quad \sigma_1=\frac{1}{3}\left(1+2\sqrt{\frac{2}{5}}\right),\ Z_1^{\pm}=-\left[1+\frac{(\sigma_1\pm\cos\theta)}{|\sigma_1\pm\cos\theta|}\mathrm{i}\right]|\sigma_1\pm\cos\theta|^{1/2}
$$

When Pr is not small, asymptotic solutions can be also obtained but their expressions are lengthy.

Asymptotic solutions valid for any P_r/E

An asymptotic solution is determined by matching u_0 to u_b at the edge of the Ekman boundary layer,

$$C_M \mathbf{i}(\sigma - \sigma_M) + \sum_N C_N \left(E\,\mathcal{F}_{MN} - R\,\mathcal{G}_{MN}\right) = -\pi E^{1/2} \sum_N C_N$$

$$\times \quad \int_0^\pi \frac{B_N^+}{\sqrt{|\sigma_N + \cos\theta|}} \left[\frac{(\sigma_N + \cos\theta)}{|\sigma_N + \cos\theta|} + \mathbf{i}\right] \left(\sin\theta \frac{\partial P_M}{\partial\theta} - mP_M\right) d\theta$$

where

$$\mathcal{F}_{MN} = \sum_{i=0}^{N} \sum_{j=0}^{N-i} \sum_{k=0}^{M} \sum_{l=0}^{M-k} \frac{C_{ijmN}}{Q_N} \frac{C_{klmM}}{Q_M} \sigma_N^{2i-1} \sigma_M^{2k-1} (1-\sigma_N^2)^{j-1} (1-\sigma_M^2)^{l-1}$$

$$\frac{(m+j+l-1)!(2i+2k-3)!!}{[2(m+j+l+i+k)-1]!!} \{8ik(2i-1)(2k-1)...(2i+2k-3)\},$$

$$P_M = \sum_{i=0}^{M} \sum_{j=0}^{M-i} \frac{2C_{ijmM}}{Q_M} \sigma_M^{2i} (1-\sigma_M^2)^j \sin^{m+2j}\theta \cos^{2i}\theta,$$

Asymptotic solutions vs. three-D numerical simulations

Pr	$(R_c, m_c, \sigma_c)_{FNUM}$	$(R_c, m_c, \sigma_c)_{QGIW}$
0.001	$(23.74, 2, -0.1064)$	$(22.14, 2, -0.1095)$
0.01	$(36.50, 2, -0.0927)$	$(35.42, 2, -0.0957)$
0.05	$(74.45, 4, -0.0466)$	$(74.65, 4, -0.0458)$
0.1	$(95.34, 5, -0.0394)$	$(94.17, 5, -0.0390)$
0.25	$(143.3, 6, -0.0269)$	$(140.8, 6, -0.0272)$
0.7	$(226.7, 7, -0.0145)$	$(225.7, 7, -0.0155)$
1.0	$(258.6, 7, -0.0108)$	$(257.9, 7, -0.0114)$

Table 1: Convection solutions at $E = 10^{-4}$ for various Prandtl numbers. The fully numerical solutions are indicated by the subscript $FNUM$ while the asymptotic solutions by the subscript $QGIW$.

Asymptotic solutions vs. three-D numerical simulations

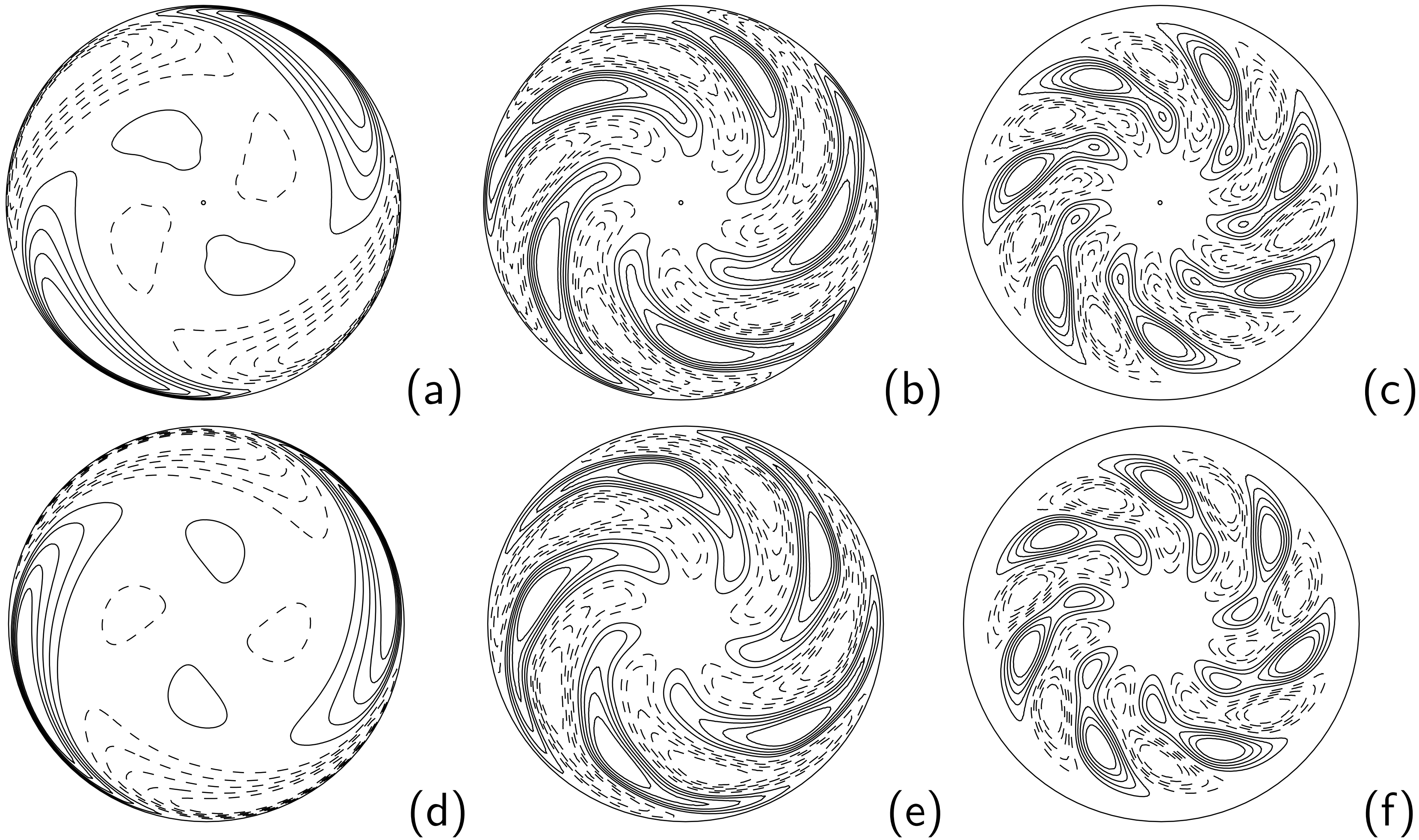

Figure 1: Contours of u_ϕ in the equatorial plane at $E = 10^{-4}$: for $P_r = 10^{-2}, 10^{-1}, 1.0$. Upper panels are numerical solutions while the lower for asymptotic solutions.

Mean flows on giant planets

Recent observations from the Hubble space telescope and the Cassini spacecraft have provided more much detailed structure and variation of the zonal flows, prograde equatorial jets and higher-latitude multiple alternating jets in the atmospheres of Jupiter and Saturn (Porco et al., 2003, 2005,; Salyk et al., 2006)). In particular, observations reveal two significant new features:

(i) A high correlation between the small-scale vortices and the mean zonal flow (the large vortex), suggesting that energy is transferred from the small vortices into the large-scale mean zonal flow via the inverse cascade;

(ii) Observations from 1996 to 2004 indicate that the equatorial jets on Saturn may have slowed substantially from over 400 m/s to about 275 m/s, suggesting that there exist strong temporal variations in the strength of the jets

Mean flows

The physical picture:

Convective instabilities $\Rrightarrow$

Small-scale correlated vortices $\Rrightarrow$

Nonlinear interaction of the vortices $\Rrightarrow$

Mean flow (the largest vortex)...

Mean flows

The new observed features, a high correlation between the small vortices and the mean flow and the strong temporal variation, prompt two fundamental questions:

(i) How to saturate the inverse cascade process, which causes a continual build up of energy in the mean flow but without a proper mechanism for dissipating it;
(ii) Whether substantial temporal variations in Saturn's equatorial jets represent a typical feature of the convection-generated mean zonal flow.

Mean flows: saturation of the inverse cascade

Making a quasi-geostrophic approximation (e.g., Gillet and Jones, 2006)in a rotating spherical annulus defined by $\eta \leq s \leq 1$, $-\sqrt{1-s^2} \leq z \leq \sqrt{1-s^2}$ and $0 \leq \phi \leq 2\pi$. In the quasi-geostrophic approximation, the vanishing vertical vorticity leads to the velocity of the convective flow being of the form

$$\mathbf{u} = \nabla \times [\hat{\mathbf{z}}\psi(s,\phi,t)] + u_z(s,\phi,z,t)\hat{\mathbf{z}}, \tag{13}$$

which lead to, after applying $\hat{\mathbf{z}} \cdot \nabla \times$

$$\frac{\partial \nabla^2 \psi}{\partial t} + \frac{1}{s}\left(\frac{\partial \psi}{\partial \phi}\frac{\partial \nabla^2 \psi}{\partial s} - \frac{\partial \psi}{\partial s}\frac{\partial \nabla^2 \psi}{\partial \phi}\right) + 2E^{-1}\frac{\partial u_z}{\partial z} = RE^{-1}\frac{\partial \Theta}{\partial \phi} + \nabla^4 \psi, \tag{14}$$

$$Pr\left[\frac{\partial \Theta}{\partial t} + \frac{1}{s}\left(\frac{\partial \psi}{\partial \phi}\frac{\partial \Theta}{\partial s} - \frac{\partial \psi}{\partial s}\frac{\partial \Theta}{\partial \phi}\right)\right] = \nabla^2 \Theta + \frac{\partial \psi}{\partial \phi} + z u_z. \tag{15}$$

The boundary condition that the normal flow vanishes on the outer spherical surface gives rise to

$$\frac{\partial \psi}{\partial \phi} + u_z\sqrt{(1-s^2)} = 0. \tag{16}$$

Saturation of the inverse cascade

Making use of the quasi-geostrophic approximation, the governing equations then reduce to

$$\frac{\partial \nabla^2 \psi}{\partial t} + \frac{1}{s}\left(\frac{\partial \psi}{\partial \phi}\frac{\partial \nabla^2 \psi}{\partial s} - \frac{\partial \psi}{\partial s}\frac{\partial \nabla^2 \psi}{\partial \phi}\right) - \frac{2}{(1-s^2)}\frac{\partial \psi}{\partial \phi} = RE^{-1}\frac{\partial \Theta}{\partial \phi} + \nabla^4 \psi, \tag{17}$$

$$Pr\left[\frac{\partial \Theta}{\partial t} + \frac{1}{s}\left(\frac{\partial \psi}{\partial \phi}\frac{\partial \Theta}{\partial s} - \frac{\partial \psi}{\partial s}\frac{\partial \Theta}{\partial \phi}\right)\right] = \nabla^2 \Theta + \frac{\partial \psi}{\partial \phi}, \tag{18}$$

which are two-dimensional nonlinear partial differential equations governing quasi-geostrophic convection in rapidly rotating spherical-shell geometry.

Saturation of the inverse cascade

Sketch of the domain decomposition

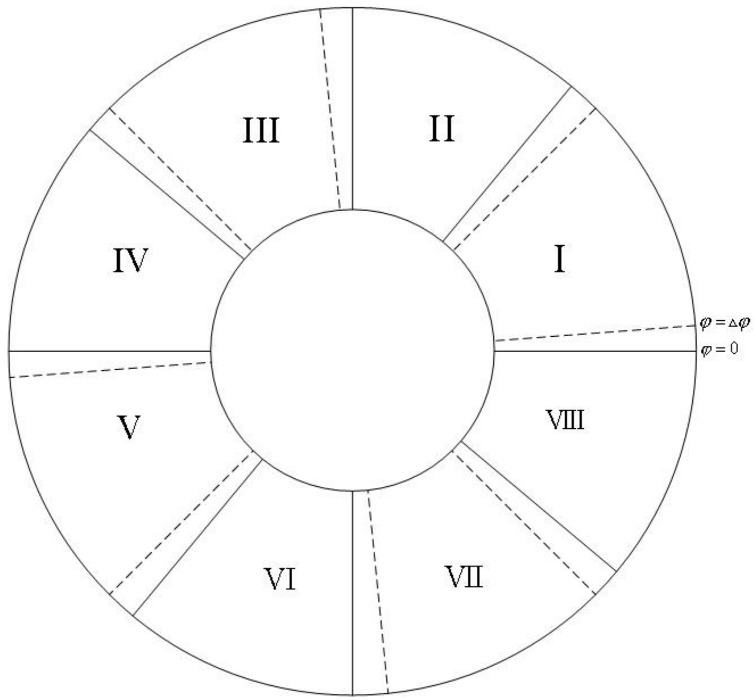

Saturation of the inverse cascade

In discussing nonlinear flows, it is convenient to introduce a supercritical Rayleigh number $\epsilon = (R - R_c)/R_c$ and to decompose the velocity of nonlinear convection into

$$\mathbf{u} = \overline{u}_\phi(s,t)\hat{\boldsymbol{\phi}} + \tilde{\mathbf{u}}(s,\phi,t),$$

where $\overline{u}_\phi$ is the mean flow and $\tilde{\mathrm{u}}$ denotes the velocity of small-scale vortices, with the corresponding averaged kinetic energies defined as

$$\bar{E}_{kin} = \frac{1}{2\pi(r_o^2 - r_i^2)} \int_0^{2\pi} \int_{r_i}^{r_o} |\overline{u}_\phi|^2 s ds d\phi; \; \tilde{E}_{kin} = \frac{1}{2\pi(r_o^2 - r_i^2)} \int_0^{2\pi} \int_{r_i}^{r_o} |\tilde{\mathbf{u}}|^2 s ds d\phi.$$

We start our numerical simulations from small values of ϵ

Saturation of the inverse cascade

Episodic convection (the secondary bifurcation)

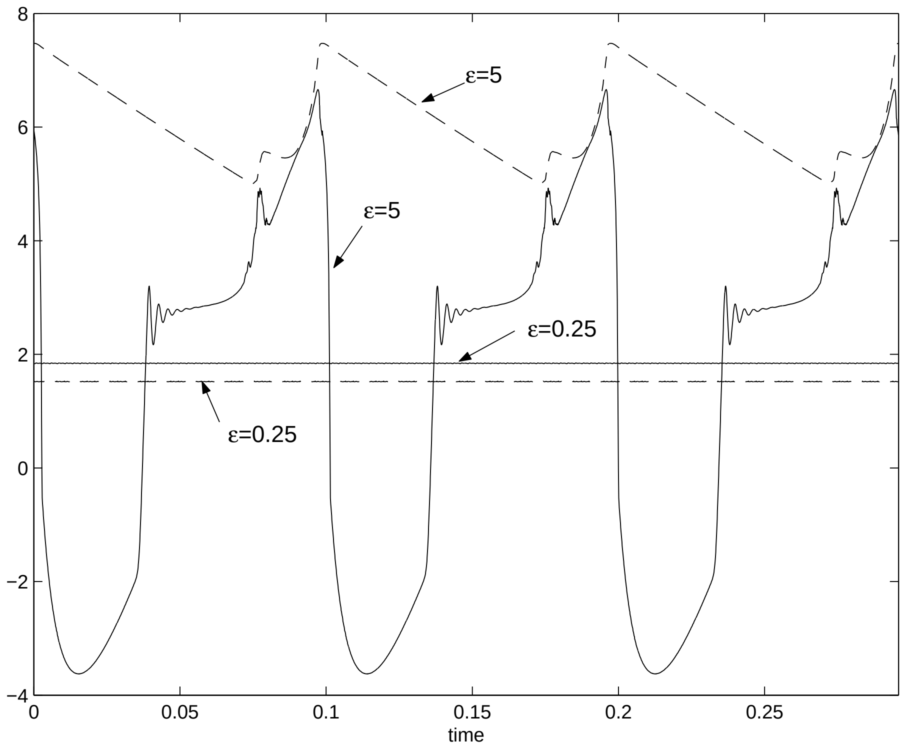

Episodic cycle for $E = 10^{-5}$ and $P_r = 1.0$ with ϵ. Dashed lines for $\bar{E}_{kin}$ while $\tilde{E}_{kin}$ by solid lines.

Planetary dynamos

The Dynamo on massively parallel computers

Sketch of geometry:

- **Inner solid core:** $0 \leq r \leq r_i$.
- **Outer fluid shell:** $r_i \leq r \leq r_o$.
- **thermally or electrically heterogeneous mantle mantle:** $r_o \leq r \leq r_m$.

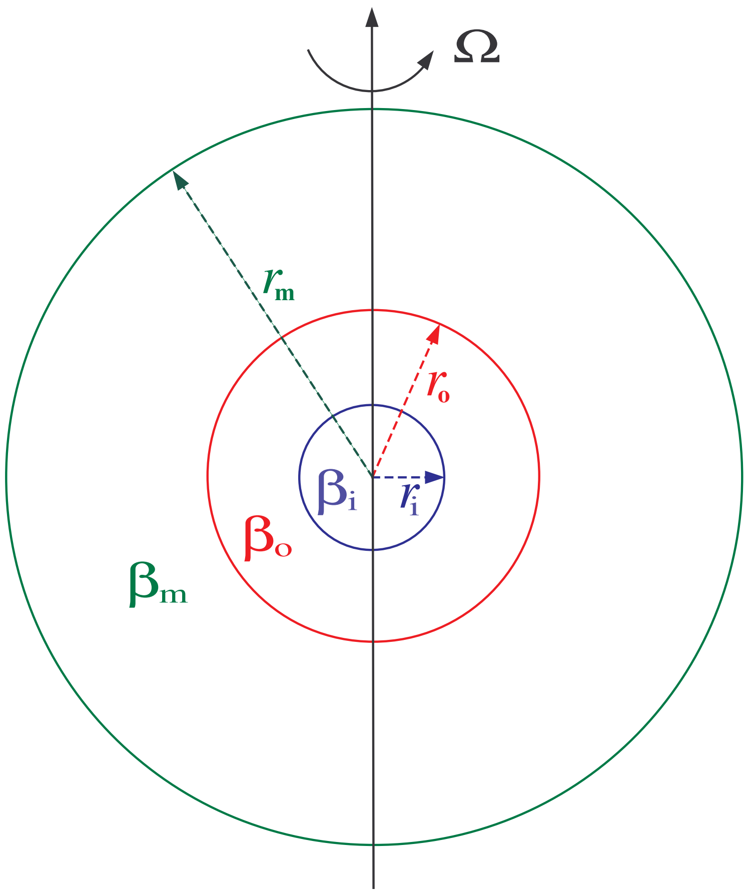

Mathematical Model

Dimensionless equations in each region:

- Fluid shell, $r_i \le r \le r_o$, generating magnetic fields

$$E\left(\frac{\partial \mathbf{u}}{\partial t} + \mathbf{u}\cdot\nabla\mathbf{u} - \nabla^2\mathbf{u}\right) + 2\hat{\mathbf{z}}\times\mathbf{u} + \nabla P = Ra\frac{\mathbf{r}}{r}\Theta + \frac{1}{Pm}(\nabla\times\mathbf{B})\times\mathbf{B}, \quad (19)$$

$$\frac{\partial \mathbf{B}}{\partial t} = \nabla\times(\mathbf{u}\times\mathbf{B}) + \frac{1}{Pm}\nabla\times\nabla\times\mathbf{B}, \quad (20)$$

$$\frac{\partial \Theta}{\partial t} + \mathbf{u}\cdot\nabla\Theta = \left(\frac{r_i r_o}{r^3}\right)\mathbf{u}\cdot\mathbf{r} + \frac{1}{Pr}\nabla^2\Theta, \quad (21)$$

$$\nabla\cdot\mathbf{u} = 0, \qquad \nabla\cdot\mathbf{B} = 0, \quad (22)$$

- The velocity and temperature boundary conditions:

$$\mathbf{u} = 0, \quad \text{at} \ \ r = r_i,\ r = r_o, \quad (23)$$

$$\Theta = 0, \quad \text{at} \ \ r = r_i,\ r = r_o. \quad (24)$$

Mathematical Model

Dimensionless equations in each region:

- Solid inner Core: $0 \leq r \leq r_i$.

$$\frac{\partial \mathbf{B}^i}{\partial t} + \beta_i \nabla \times \nabla \times \mathbf{B}^i = 0, \tag{25}$$

$$\nabla \cdot \mathbf{B}^i = 0, \tag{26}$$

$$\mathbf{B}^i - \mathbf{B} = \mathbf{r} \times \left(\beta_i \nabla \times \mathbf{B}^i - \frac{1}{Pm} \nabla \times \mathbf{B} \right) = 0, \quad \text{at} \;\; r = r_i. \tag{27}$$

- Solid mantle: $r_o \leq r \leq r_m$.

$$\frac{\partial \mathbf{B}^e}{\partial t} + \nabla \times (\beta_m(\mathbf{r}) \nabla \times \mathbf{B}^e) = 0, \tag{28}$$

$$\nabla \cdot \mathbf{B}^e = 0, \tag{29}$$

$$\mathbf{B} - \mathbf{B}^e = \mathbf{r} \times \left(\frac{1}{Pm} \nabla \times \mathbf{B} - \beta_m(\mathbf{r}) \nabla \times \mathbf{B}^e \right) = 0, \quad \text{at} \;\; r = r_o. \tag{30}$$

$$\mathbf{B}^e = 0, \quad \text{at} \;\; r = r_m. \tag{31}$$

Tetrahedral spherical FEM Mesh:

No pole and origin problems

Particularly suitable for modern massively parallel computers.

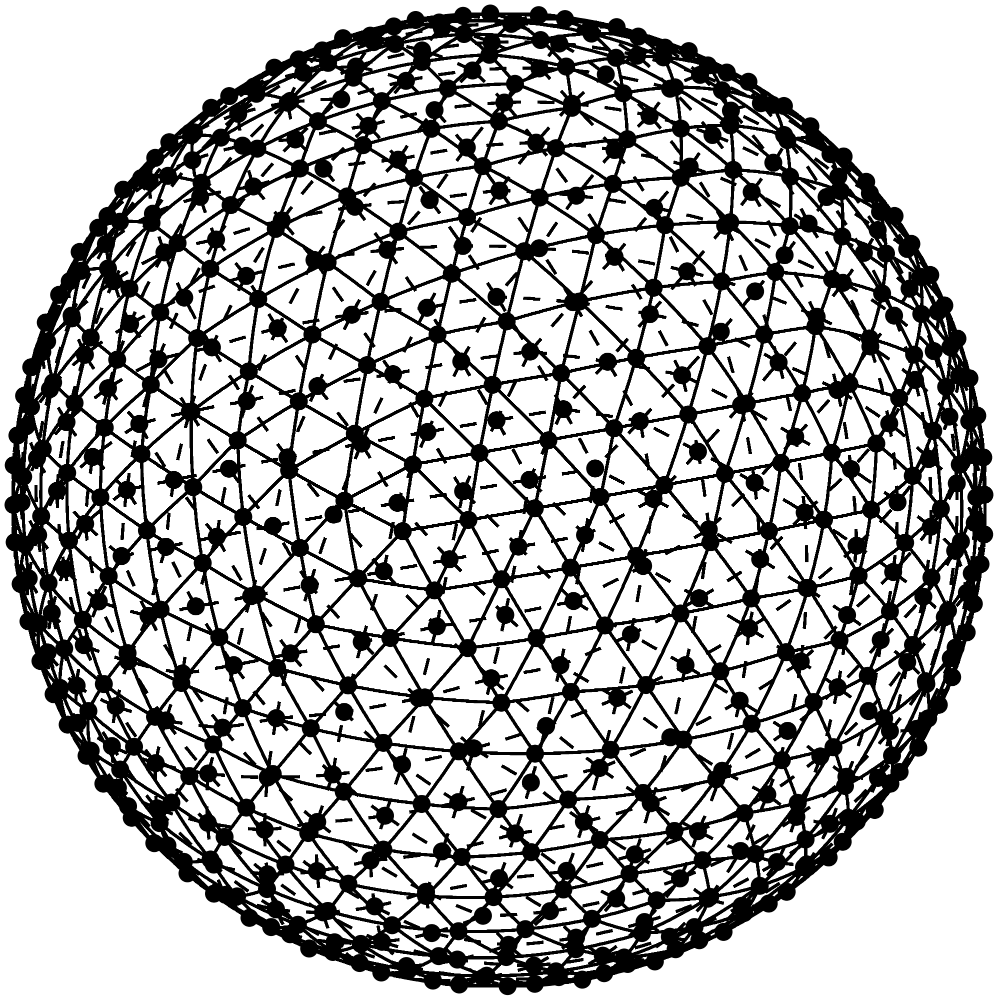

Tetrahedral spherical FEM Mesh:

No pole and origin problems

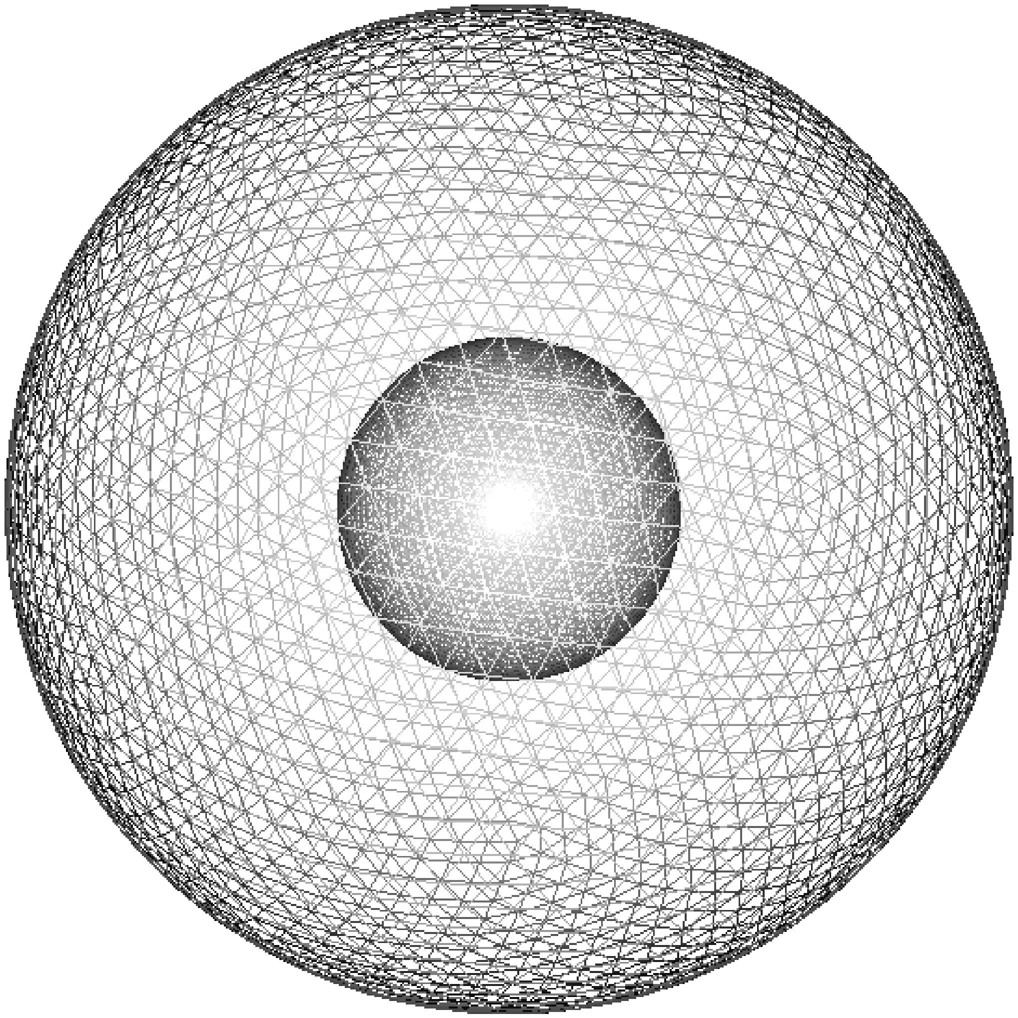

Tetrahedral spherical FEM Mesh:

No pole and origin problems

Particularly suitable for modern massively parallel computers.

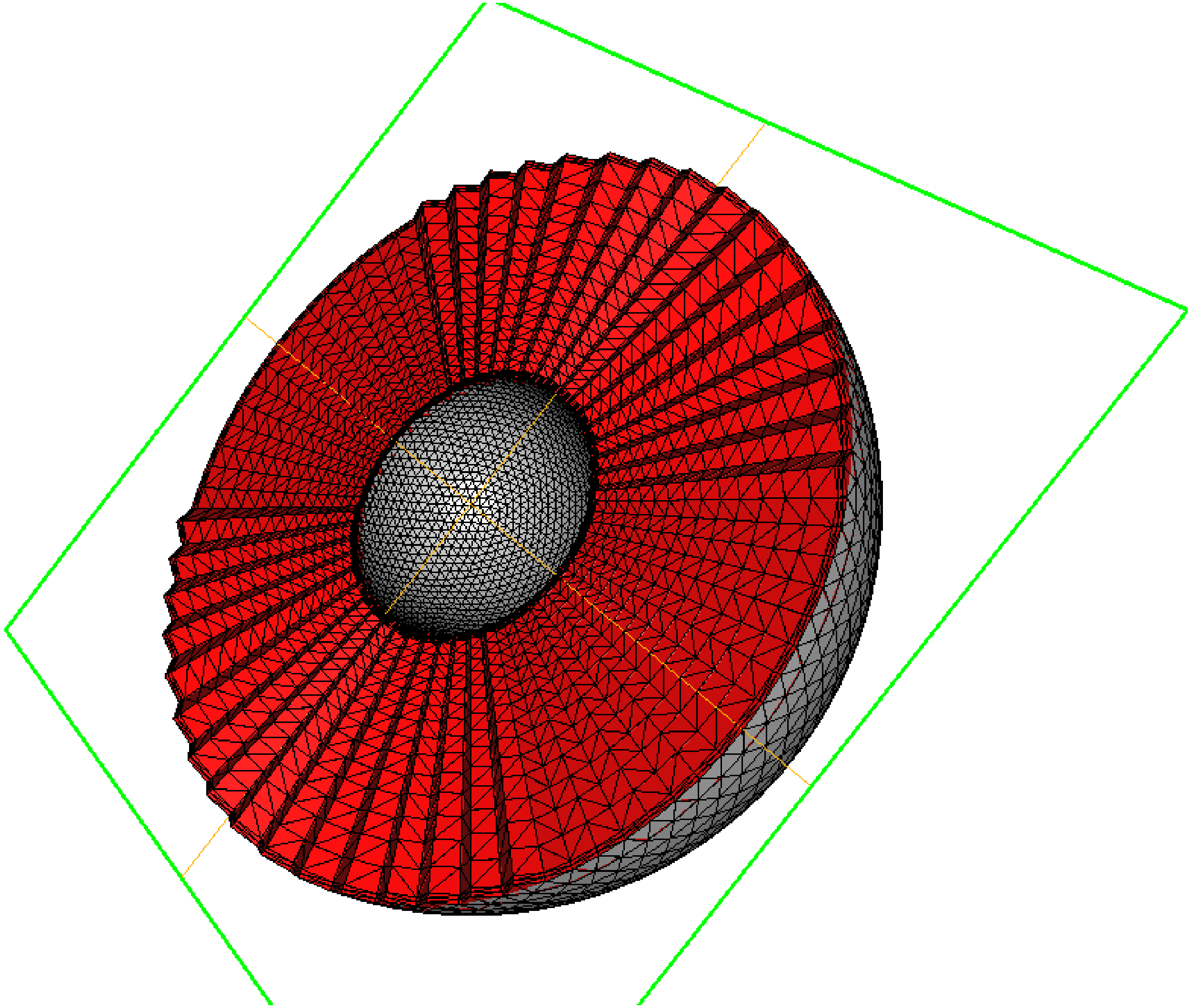

Parallel Dynamo Simulations

- **Element-by-element (EBE)** parallelization technique adopted.
- Fortran 90 code with Message Passing Interface (MPI).
- Reproduce the spectral dynamo benchmark.

- **The nearly linear scalability of the parallel code.**
- **The existence/convergence of the numerical scheme is proved by Chan, Zhang and Zou (2006, SIAM J. Numer. Anal.)**

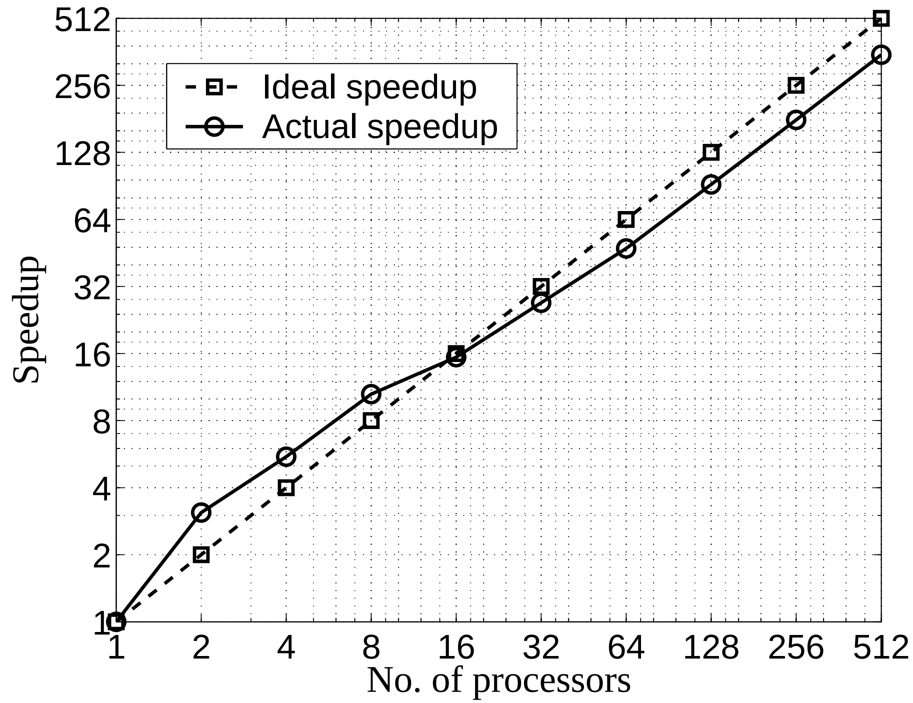

Geomagnetic fields: simulations

The radial field at the core-mantle boundary at two instants for m=2.